

Three-Dimensional Speckle-Tracking Echocardiographic Monitoring of Acute Rejection in Heart Transplant Recipients

Guo-Qing Du, MD, Ming-Chon Hsiung, MD, Yan Wu, MD, Shao-Hui Qu, MD, Jeng Wei, MD, Wei-Hsian Yin, MD, Jia-Wei Tian, MD

Received July 7, 2015, from the Department of Ultrasound, Second Affiliated Hospital of Harbin Medical University, Harbin, China (G.-Q.D., Y.W., S.-H.Q., J.-W.T.); Key Laboratories of Myocardial Ischemia Mechanism and Treatment, Harbin Medical University, Ministry of Education, Harbin, China (G.-Q.D., Y.W., S.-H.Q., J.-W.T.); Division of Cardiology, Heart Center, Cheng Hsin General Hospital, Taipei, Taiwan (M.-C.H., J.W., W.-H.Y.); and Faculty of Medicine, National Yang-Ming University, Taipei, Taiwan (W.-H.Y.). Revision requested August 10, 2015. Revised manuscript accepted for publication September 1, 2015.

We thank Nathan C. Ni, PhD, for assistance with manuscript preparation. Part of this work was financially supported by the National Natural Science Foundation of China (grant 81371632). Drs Du and Hsiung contributed equally to this work.

Address correspondence to Jia-Wei Tian, MD, Department of Ultrasound, Second Affiliated Hospital of Harbin Medical University, 246 Xuefu Rd, Nangang District, 150086 Harbin, China.

E-mail: jiaweitian@126.com

Abbreviations

ICC, intraclass correlation coefficient; ISHLT, International Society for Heart and Lung Transplantation; LV, left ventricular; LVEF, left ventricular ejection fraction; 3D, 3-dimensional; 2D, 2-dimensional

doi:10.7863/ultra.15.07013

Objectives—This study assessed the use of 3-dimensional (3D) speckle-tracking echocardiography for noninvasive monitoring and diagnosis of acute rejection in heart transplant recipients.

Methods—Fifteen heart transplant recipients underwent 32 endomyocardial biopsies; echocardiography was performed within 3 hours before biopsy. Twenty-four biopsies (acute rejection–negative group) showed grade 0 or 1A rejection, and 8 biopsies (acute rejection–positive group) showed grade 1B or higher rejection (based on the International Society for Heart and Lung Transplantation criteria). Two-dimensional, M-mode, pulsed Doppler, and tissue Doppler echocardiography were performed to assess conventional heart structure and function, and 3D full-volume echocardiography was recorded and analyzed.

Results—Global peak longitudinal strain was significantly lower in the acute rejection–negative group compared to the positive group (mean \pm SD, $-7.38\% \pm 1.34\%$ versus $-10.88\% \pm 3.81\%$; $P = .017$). Differences in left ventricular global peak radial strain ($28.79\% \pm 10.79\%$ versus $24.32\% \pm 5.24\%$; $P = .272$), global peak circumferential strain ($-12.16\% \pm 4.87\%$ versus $-12.61\% \pm 2.38\%$; $P = .806$), and ejection fraction ($49.42\% \pm 12.17\%$ versus $50.68\% \pm 7.26\%$; $P = .824$) between the negative and positive groups were not significant. Significant correlations were observed between the left ventricular ejection fraction and global peak longitudinal, global peak radial, and global peak circumferential ($r = -0.72$; $P < .001$; $r = 0.60$; $P < 0.001$; and $r = -0.69$; $P < 0.001$, respectively). Receiver operating characteristic curve analysis showed that a global peak longitudinal strain cutoff value of less than -9.55% could predict grade 1B or higher rejection with sensitivity of 87.50% and specificity of 54.17%.

Conclusions—Three-dimensional speckle-tracking echocardiography–derived global peak longitudinal strain is a useful parameter for detecting acute rejection; thus, 3D speckle-tracking echocardiography can monitor dynamic and acute rejection ($\geq 1B$) in heart transplant recipients.

Key Words—acute rejection; echocardiography; heart transplant; 3-dimensional speckle-tracking echocardiography

Although incidences of acute rejection in heart transplant recipients have been substantially reduced by the use of advanced immunosuppressive therapy,¹ acute rejection can cause allograft vasculopathy and elevate the risk of heart failure.²

Therefore, evaluating cardiac function and detecting acute rejection are essential after heart transplantation. The reference-standard method for diagnosing rejection in cardiac transplantation is endomyocardial biopsy. However, this procedure is invasive, expensive, and subject to sampling errors and interobserver variability.^{3,4} Many non-invasive techniques have been used to detect cardiac transplant rejection in clinical trials, such as magnetic resonance imaging,⁵ radionuclide imaging,⁶ 2-dimensional (2D) ultrasonic myocardial integrated backscatter,⁷ and gene expression profiling,^{8,9} but none of them have been considered sufficiently accurate for early diagnosis of acute rejection or sufficiently effective for replacing endomyocardial biopsy.

Echocardiography is a noninvasive technique that has shown early promise in correlating functional changes associated with biopsy-confirmed acute rejection.¹⁰ Conventionally, ventricular volumes, the ejection fraction, and Doppler assessment of hemodynamics are used to evaluate left ventricular (LV) systolic function of heart transplant recipients via 2D, M mode, and stress echocardiography.^{11–15} The parameters obtained from conventional echocardiography are useful for detecting LV dysfunction associated with acute rejection. However, they are not sufficiently sensitive for detecting abnormalities in clinically stable patients; thus, treatment of asymptomatic patients may not be properly guided by these existing parameters. Tissue Doppler imaging has shown better accuracy in detecting acute rejection than conventional echocardiography. Sun et al¹⁶ compared 2D and tissue Doppler echocardiography and found that the isovolumic relaxation time (<90 milliseconds) and pulsed Doppler early-to-late diastolic velocity ratio (>1.7) were significant predictors of acute cardiac allograft rejection. In the experience of Stengel et al,¹⁷ the late diastolic transmitral peak velocity derived from tissue Doppler imaging showed good sensitivity of 82% but low specificity of 53% in predicting significant heart transplant rejection. Finally, Sachdeva et al¹⁸ found that septal systolic velocity and tricuspid annular late diastolic velocity of the mitral annulus were associated with rejection but had low sensitivity and specificity. An elevated lateral early diastolic transmitral peak velocity-to-early diastolic mitral annular velocity ratio did not predict rejection. They suggested that tissue Doppler imaging was insensitive and ineffective for marking early myocardial dysfunction and should be limited to assessing changes in ventricular cavity size during the cardiac cycle.

Speckle-tracking echocardiography is a novel tool for assessment of strain, which has the capability to examine LV myocardial dysfunction cardiovascular disease. Two-

dimensional longitudinal strain and the strain rate are used to analyze myocardial deformation by tracking speckles (natural acoustic markers) throughout the cardiac cycle. Strain is a measure of deformation, an intrinsic mechanical property, which denotes the percentage of thickening or deformation of the myocardium during the cardiac cycle and measures myocardial systolic function more directly compared to conventional cavity-based echocardiographic measures. Strain echocardiography has been introduced as an accurate tool for assessment of global and regional LV myocardial function.¹⁹

Speckle-tracking echocardiography can track image speckles from frame to frame to quantify cardiac motion.²⁰ Many studies have been done to evaluate the value of 2D speckle-tracking echocardiography for assessment of cardiac systolic/diastolic function and detection of acute rejection in heart transplant recipients.^{21–24} They demonstrated that 2D speckle-tracking echocardiography might be a good tool for detecting grade 1B or higher acute rejection in heart transplant recipients. However, most speckle-tracking echocardiographic techniques derived from 2D echocardiography focused on 3 apical views (4-, 3-, and 2-chamber views) and lacked assessment of the entire LV deformation. Three-dimensional (3D) speckle-tracking echocardiography is a promising method for assessment of cardiac function using complete 3D pyramidal data sets. It has been suggested that the 3D speckle-tracking echocardiography might be more accurate than conventional and 2D speckle-tracking echocardiography for assessment of LV function.^{25,26} This concept is based on the fact that 2D algorithms only track speckles in 2D planes, whereas speckles move in 3 dimensions; therefore, only a portion of the real motion can be detected.²⁶ Despite this fact, few researchers have used 3D speckle-tracking echocardiography to evaluate the myocardial mechanics underlying cardiac allograft rejection.

In this study, we used conventional echocardiography and 3D speckle-tracking echocardiography to analyze the myocardial deformations of heart transplant rejection and to assess the utility of 3D speckle-tracking echocardiography as a noninvasive technique for diagnosis of rejection.

Materials and Methods

Patients

Fifteen heart transplant recipients (13 men and 2 women) who underwent endomyocardial biopsy at 1-year intervals or when rejection was suspected were recruited from the Cheng Hsin General Hospital. Serial right ventricular

endomyocardial biopsies were performed through the right jugular vein using a Swan-Ganz thermodilution catheter according to the regular practices of our institution. The Taiwan Research Ethics Committee approved this protocol, and written informed consent was given by all patients.

We classified acute rejection using the diagnosis of cellular acute rejection, based on conventional International Society for Heart and Lung Transplantation (ISHLT) criteria.²⁷ Since rejection grades 0 and 1A need not receive treatment in standard clinical practice, biopsy specimens showing ISHLT grades 0 and 1A were assigned to an acute rejection–negative group. Accordingly, samples showing grade 1B or higher rejection were assigned to an acute rejection–positive group. A series of echocardiographic examinations were made to monitor changes in LV strain after the positive group patients received augmented immunosuppression. An experienced pathologist, who was blinded to the clinical diagnosis and echocardiograms, graded the histologic results.

Echocardiography

Conventional echocardiography and 3D speckle-tracking echocardiography were performed within 3 hours before endomyocardial biopsy. All of the 2D echocardiographic studies were performed with a commercial scanner (Acuson SC2000; Siemens Medical Solutions, Mountain View, CA). Standard comprehensive M-mode, 2D echocardiographic, and Doppler studies were performed. Interventricular septal thickness, LV posterior wall thickness, and LV end-systolic and end-diastolic diameters were measured by M-mode echocardiography. Early and late diastolic flow velocities were obtained by placing a flow Doppler sample volume at the tips of the mitral valve leaflets.

Tissue Doppler Echocardiography

Systolic and diastolic excursions of the mitral annulus were obtained by placing a tissue Doppler sample volume at the septal and lateral mitral annuli in the apical 4-chamber view, using a 2D-guided pulsed tissue Doppler cursor. All measurements were documented at a sweep rate of 100 mm/s, and the gain was minimized to allow for a clear tissue signal with minimum background noise. Peak systolic, early diastolic, and late diastolic mitral annular excursion velocities in the longitudinal axis were measured offline.

Three-Dimensional Speckle-Tracking Echocardiography

Images were obtained from an apical position by using a 3D transthoracic transducer. In the tissue harmonic mode, full-volume acquisitions were recorded, consisting of 4

wedge-shaped subvolumes acquired by single-beat capture. The depth and sector width were adjusted to improve the temporal and spatial resolution of the images and ensure that the entire left ventricle remained within the pyramidal volume.

An experienced investigator, who was blinded to the patient's clinical diagnosis and the results obtained from standard echocardiography, analyzed the data by using Siemens analysis software. After semiautomated tracing of the endocardial and epicardial borders, the software automatically analyzed the entire cardiac cycle and provided LV global peak longitudinal strain, global peak radial strain, and global peak circumferential strain values (Figure 1, A and B). Longitudinal, radial, and circumferential strain values indicate myocardial deformation. Longitudinal strain refers to myocardial shortening in the longitudinal direction (a negative value indicates shortening). Radial strain refers to myocardial excursion in the direction toward the endocardial surface (a positive value indicates displacement toward the center of the cavity). Circumferential strain refers to myocardial shortening in the short-axis direction toward the endocardial contour (a negative value indicates shortening). Tissue synchronization imaging of the left ventricle was also performed (Figure 1C). The LV end-diastolic volume, LV end-systolic volume, and LV ejection fraction (LVEF) were obtained simultaneously.

Interobserver and Intraobserver Reproducibility

To examine intraobserver variability, the same observer analyzed the same data twice 1 week apart and was blinded to all prior results. To test interobserver variability, the same 3D data were evaluated by 2 sonographers blindly. Intraclass correlation coefficients (ICCs) were used to assess the reproducibility of the 3D global strain values. Reproducibility of the results was expressed as a coefficient of variation between the 2 measurements.

Statistical Analysis

Continuous data are presented as mean \pm standard deviation. Echocardiographic indices and hemodynamic variables were compared between groups by Student *t* test analysis. Linear regression was conducted to determine possible agreement between continuous variables. Reliability was assessed by the ICC. To determine the ICC, different variance components were calculated by the restricted maximum likelihood method of estimation and a model for absolute agreement, in which the observers and patients (or segments) were entered as random effects. The clinical significance of the ICC was interpreted as follows: good, 0.75 or greater; moderate, 0.40 to 0.75; and poor, less than 0.40.²⁸

The ICCs were expressed as percentages. The optimal cut-off values of individual parameters for differentiation between acute rejection–positive and –negative groups were determined by a receiver operating characteristic curve. Statistical significance was defined as $P < .05$. Data were analyzed with SPSS version 19.0 software (IBM Corporation, Armonk, NY).

Results

Patient Characteristics and Clinical Data

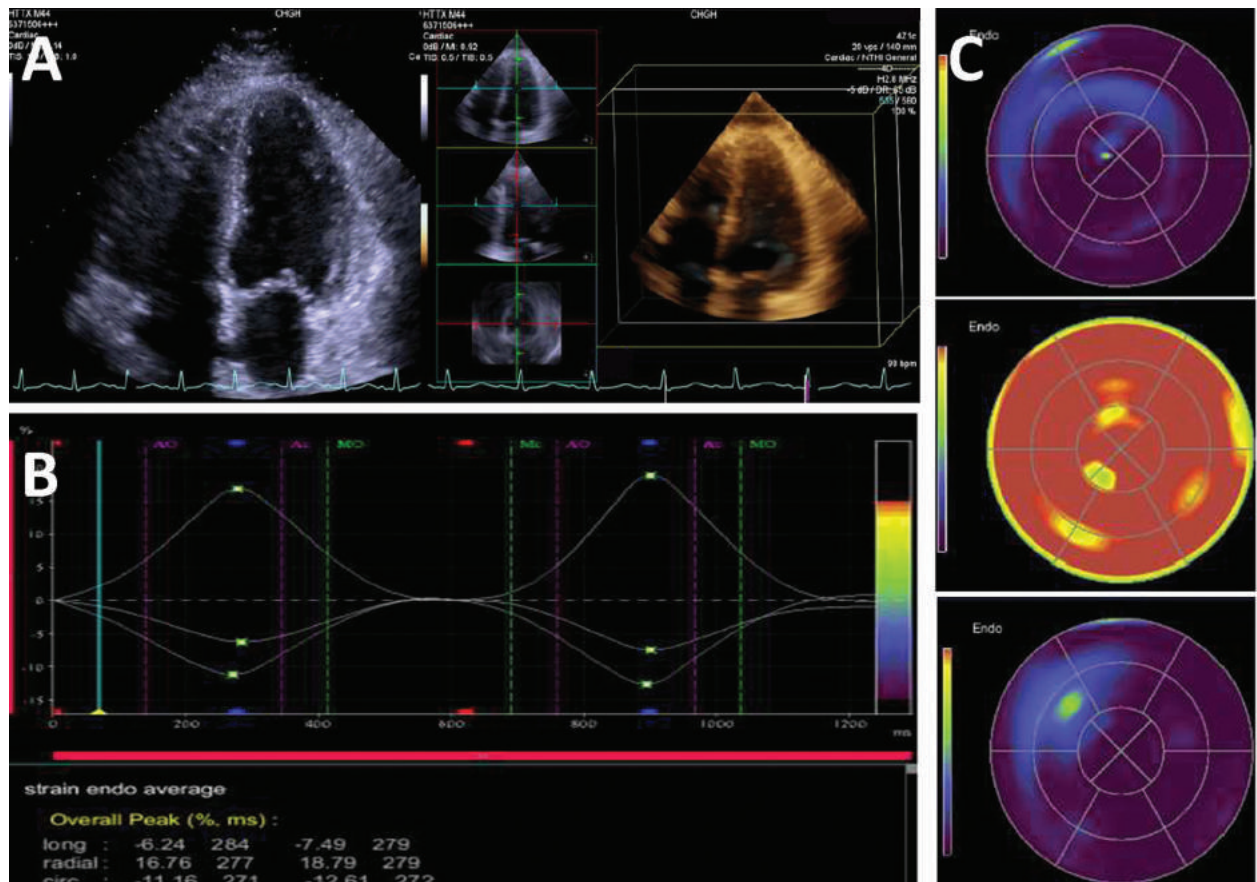
Among the 32 endomyocardial biopsy procedures performed in this study (ranging from 1–5 biopsies per patient), 4 biopsies (12.5%) showed conventional ISHLT grade 0; 20 (62.5%) showed grade 1A; 5 (15.6%) showed grade 1B; 1 (3.13%) showed grade 2; and 2 (6.25%) showed grade 3A. Thus, 24 examinations were assigned to the acute rejection–negative group, and 8 were assigned to the acute rejection–positive groups.

The characteristics of the patient groups are summarized in Table 1. The donor heart age, reason for transplantation, systolic and diastolic blood pressures, and heart rate showed no significant differences between the groups.

Two- and Three-Dimensional Echocardiographic Parameters

Conventional echocardiographic parameters are summarized in Table 2. M-mode echocardiographic and Doppler flow velocity parameters showed no significant differences between the negative and positive groups. We found significant differences between the groups for the early diastolic velocity of the lateral mitral annulus and late diastolic velocity of the septal mitral annulus. There were no significant differences between the groups for the other mitral and tricuspid annular motion velocities.

Figure 1. **A**, Representative 3D images obtained from an apical position. **B**, Curves and results for LV global longitudinal, radial, and circumferential strain. **C**, Representative bull's-eye maps of longitudinal (top), radial (middle), and circumferential (bottom) global strain in a healthy participant.



Three-dimensional echocardiographic parameters are shown in Table 3. The LV end-diastolic volume was significantly larger in the positive group compared to the negative group, whereas there were no significant differences between the groups for the LV end-systolic volume and LVEF.

Table 1. Clinical Characteristics

Characteristic	AR ⁻	AR ⁺	P
Patients, n	7	8	NA
Endomyocardial biopsies, n	24	8	NA
Age, y	53 ± 9	50 ± 11	.733
Follow-up after heart transplant, d	457 ± 35	423 ± 58	.642
Reason for heart transplant, n			NA
Coronary artery disease	2	1	NA
Dilated cardiomyopathy	3	4	NA
Valvar heart disease	1	1	NA
Other	1	2	NA
Systolic blood pressure, mm Hg	132 ± 8	129 ± 9	.656
Diastolic blood pressure, mm Hg	82 ± 5	86 ± 9	.774
Heart rate, beats/min	90 ± 9	93 ± 12	.803

Data are expressed as mean ± SD where applicable. AR indicates acute rejection; and NA, not applicable.

Table 2. Conventional Echocardiographic Parameters for Acute Rejection—Negative and —Positive Groups

Parameter	AR ⁻	AR ⁺	P
M-mode			
IVST, mm	11.90 ± 1.20	11.40 ± 1.50	.786
LVPWT, mm	12.60 ± 1.90	11.90 ± 1.30	.801
LVEDD, mm	92.70 ± 24.10	116.10 ± 30.20	.354
LVESD, mm	48.30 ± 19.40	57.80 ± 19.40	.433
Transmitral Doppler			
E, m/s	0.84 ± 0.33	0.78 ± 0.25	.186
A, m/s	0.55 ± 0.27	0.49 ± 0.32	.233
E/A	1.47 ± 0.68	1.59 ± 0.34	.122
Tissue Doppler			
LV lateral mitral annulus			
S', cm/s	10.59 ± 2.59	10.07 ± 3.57	.660
E', cm/s	13.78 ± 4.29	10.09 ± 2.99	.033
A', cm/s	6.53 ± 2.09	7.44 ± 2.93	.354
LV septal mitral annulus			
S', cm/s	6.99 ± 1.38	6.76 ± 1.85	.715
E', cm/s	7.19 ± 1.64	6.99 ± 1.85	.774
A', cm/s	4.68 ± 1.49	6.22 ± 1.44	.020

Data are expressed as mean ± SD. A indicates late diastolic transmitral peak velocity; A', late diastolic velocity of the mitral annulus; AR, acute rejection; E, early diastolic transmitral peak velocity; E', early diastolic velocity of the mitral annulus; E/A, early-to-late diastolic velocity ratio; LVEDD, LV end-diastolic diameter; LVESD, LV end-systolic diameter; IVST, interventricular septum thickness; LVPWT, LV posterior wall thickness; and S', systolic velocity of the mitral annulus.

Three-Dimensional Speckle-Tracking Echocardiography–Derived LV Strain

Three-dimensional speckle-tracking echocardiography–derived global peak longitudinal strain was significantly lower in the positive group compared to the negative group, whereas there were no significant differences between the groups for global peak radial and circumferential strain (Table 3). Bull’s-eye maps show a time to peak systolic strain in the negative group that was similar in all segments that reached peak systolic strain, in contrast to the positive group, which showed asynchronization (Figure 2). Significant correlations were seen between 3D speckle-tracking echocardiography–derived global peak longitudinal strain and the LVEF ($r = -0.72$; $P < .001$). For global peak radial and circumferential strain, correlations were found with the LVEF ($r = 0.60$; $P < .001$; and $r = -0.69$; $P < 0.001$, respectively), as shown in Figure 3.

Receiver operating characteristic curve analysis showed that global peak longitudinal strain was a good parameter for predicting grade 1B or higher rejection ($P = .019$). However, there was no significant correlation between global peak radial strain and the LVEF or global peak circumferential strain and the LVEF for prediction of grade 1B or higher rejection (Figure 4). Using a global peak longitudinal strain cutoff value of less than -9.55% for the presence of grade 1B or higher rejection yielded sensitivity of 87.50% and specificity of 54.17%.

As shown in Figure 5, serial 3D echocardiography was performed for monitoring the changes in the LVEF and 3D global strain in 5 patients from the positive group (4 men and 1 woman) before and after augmented immunosuppression. After augmented immunosuppressive therapy, LVEF and 3D global strain values were improved immediately, indicating that 3D speckle-tracking echocardiography can dynamically monitor development of acute rejection ($\geq 1B$) in heart transplant recipients.

Table 3. Left Ventricular 3D Echocardiographic Parameters for Acute Rejection—Negative and —Positive Groups

Parameter	AR ⁻	AR ⁺	P
LVEDV, mL	92.75 ± 24.12	116.10 ± 30.24	.034
LVESV, mL	48.30 ± 19.42	57.80 ± 19.38	.240
LVEF, %	49.42 ± 12.17	50.68 ± 7.26	.786
GPLS, %	-10.88 ± 3.81	-7.38 ± 1.34	.017
GPRS, %	28.79 ± 10.79	24.32 ± 5.24	.272
GPCS, %	-12.16 ± 4.87	-12.61 ± 2.38	.806

Data are expressed as mean ± SD. AR indicates acute rejection; GPCS, LV global peak circumferential strain; GPLS, LV global peak longitudinal strain; GPRS, LV global peak radial strain; LVEDV, LV end-diastolic volume; and LVESV, LV end-systolic volume.

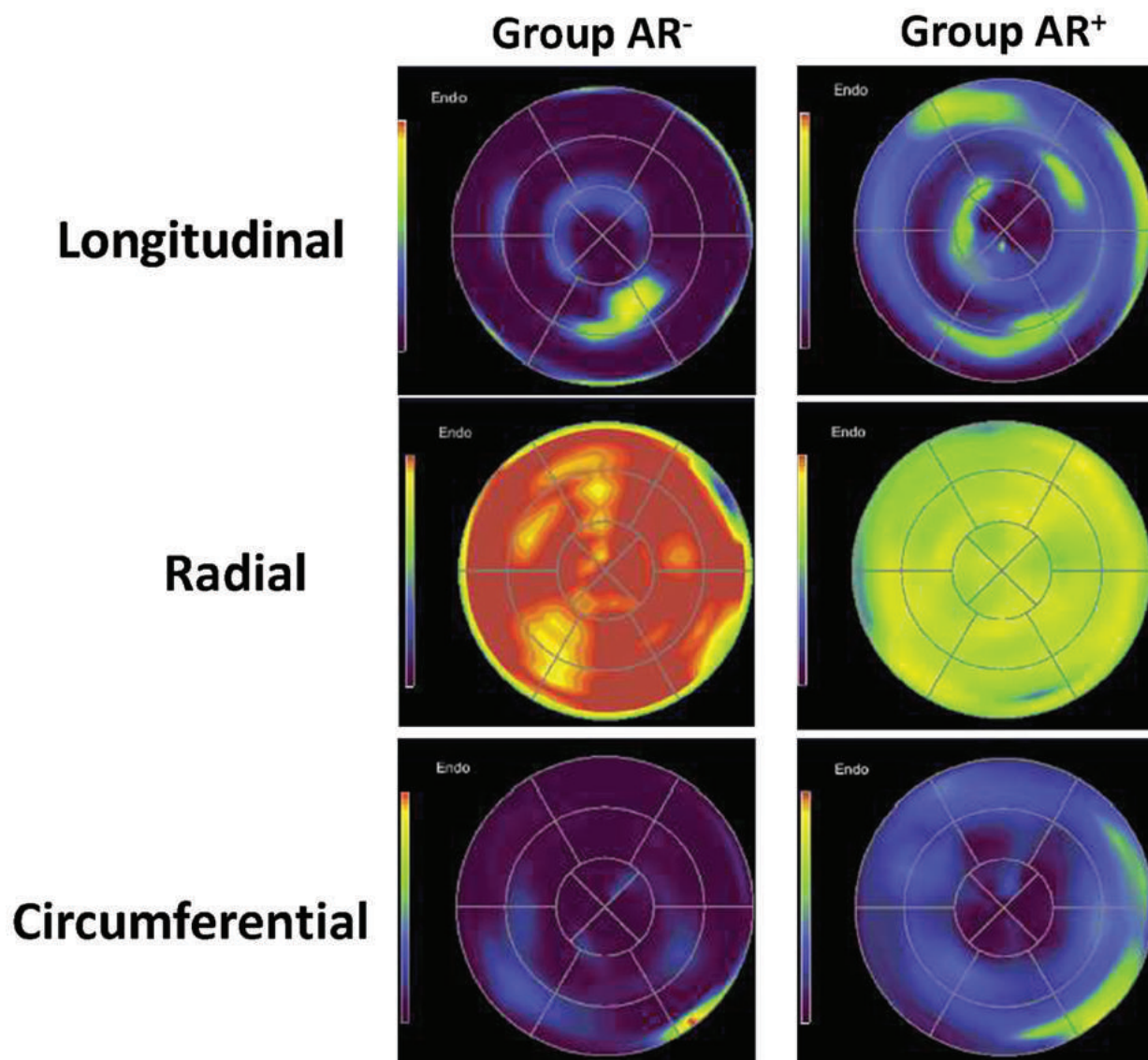
Intraobserver and Interobserver Variability

The ICC values for intraobserver reproducibility of strain analysis were 0.95, 0.92, and 0.94 for global peak longitudinal, radial, and circumferential strain, respectively. The interobserver reproducibility was also excellent, with ICC values of 0.93, 0.90, and 0.92 for global peak longitudinal, radial, and circumferential strain.

Discussion

Cardiac parameters derived from conventional and 2D speckle-tracking echocardiography have been used to assess acute rejection after transplantation and address the correlation with endomyocardial biopsy-determined rejection grades in a number of recent studies.^{16,17,21–24}

Figure 2. Bull's-eye maps of longitudinal, radial, and circumferential segmental strain in acute rejection-negative (AR-) and acute rejection-positive (AR+) groups. The different colors in the color bar represent myocardial motion in different directions. The movement of the LV myocardium in the AR+ group showed substantial tissue asynchronization, whereas that in the AR- group showed good tissue synchronization.



However, few researchers have used 3D speckle-tracking echocardiography to evaluate the myocardial mechanics in cardiac allograft rejection and examine the relationship between endomyocardial biopsy rejection grades and echocardiography-derived cardiac deformation parameters.

The main findings of this study were as follows: (1) Global peak longitudinal strain derived from 3D speckle-tracking echocardiography showed a significant difference between acute rejection-positive and -negative groups. However, the groups did not differ with respect to global peak radial and circumferential strain values. (2) Global peak longitudinal, circumferential, and radial strain all showed a good correlation with the LVEF. (3) Global peak longitudinal strain was an independent predictor of grade 1B or

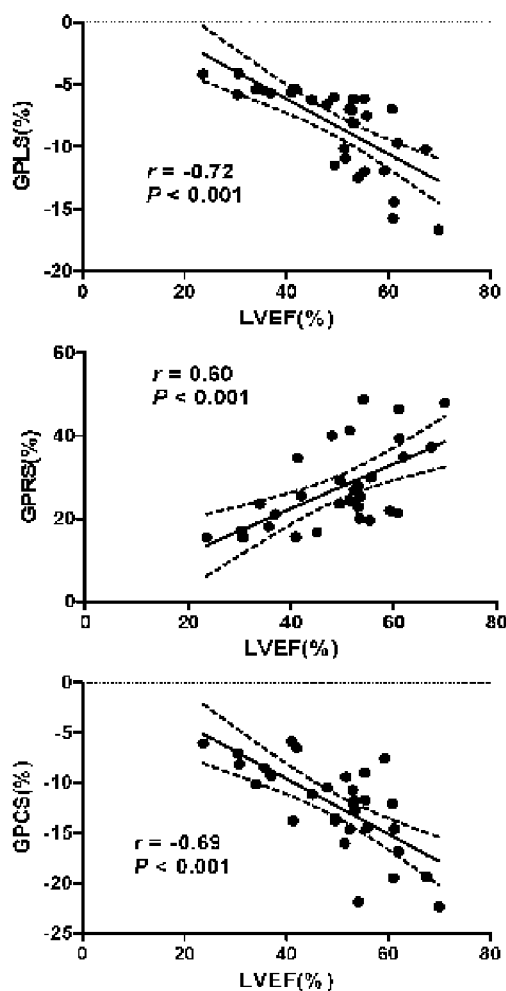
higher rejection for heart transplant recipients. The optimal cutoff value was less than -9.55% for predicting grade 1B or higher rejection with sensitivity of 87.50% and specificity of 54.17% .

The lack of any statistical differences between the positive and negative groups confirmed that the variables obtained from conventional echocardiography have relatively low sensitivity for detecting acute rejection.¹⁰ Tissue Doppler echocardiography is a technique used to detect the velocity of regional myocardial motion. However, the values obtained from heart transplant recipients are markedly influenced by the exaggerated overall motion of the heart.¹⁸ In our study, we found significant differences in the early diastolic velocity of the lateral mitral annulus and late diastolic velocity of the septal mitral annulus between the positive and negative groups. Our results were similar to those of Stengel et al,¹⁷ which suggested that a reduced late diastolic mitral annular motion velocity cannot predict severe rejection effectively because it is not specific enough.

During acute rejection, inflammatory cells penetrate the parenchymal tissues, resulting in interstitial edema and subsequent injury to the cardiomyocyte fibers, which can affect myocardial contractile function.²⁹ Torrent-Guasp et al³⁰ found that myocardial muscle fibers are arranged in spiral orientations, which can be roughly divided into longitudinal, circumferential, and oblique conformations from endocardium to epicardium. In our study, 3D speckle-tracking echocardiography traced the motion of the endocardium so an impaired longitudinal direction of LV contractile function could be detected at an early stage. When contractile function of endocardial muscle fibers is damaged, other layers of the heart wall may show compensatory enhanced motion.²⁶ This factor may explain the finding that only global peak longitudinal strain derived from 3D speckle-tracking echocardiography, but not global peak radial and circumferential strain, showed a significant association with acute rejection.

Certainly, a reduction in strain values in transplanted hearts might not be specific to rejection but also might be caused by other pathophysiologic changes, such as ischemic injury and surgical stress. In this study, we found that the degree of strain decline was associated with the rejection grade, and we could also monitor strain value changes during the process of augmented immunosuppression by serial echocardiography. This factor is especially helpful for patients who are asymptomatic but require confirmation of any possible risk of rejection when withdrawing from steroid therapy, changing their immunosuppressive regimen, or recovering from infection and in cases of post-transplant proliferative lymph disorder.

Figure 3. Correlation between the LVEF and LV global peak longitudinal strain (GPLS), global peak radial strain (GPRS), and global peak circumferential strain (GPCS). All strain parameters showed a good correlation with the LVEF ($P < 0.001$).



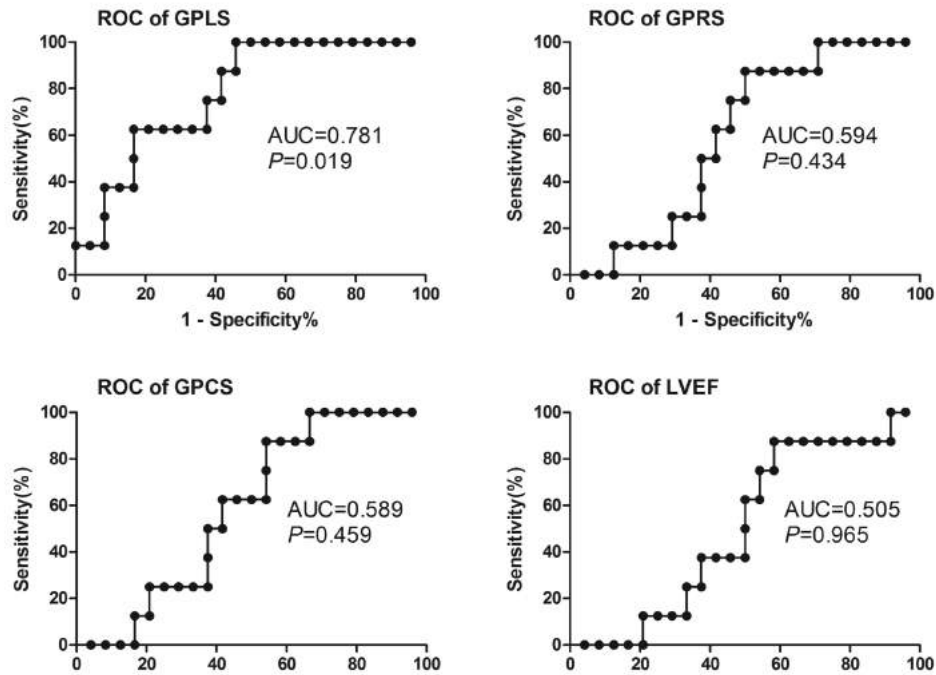
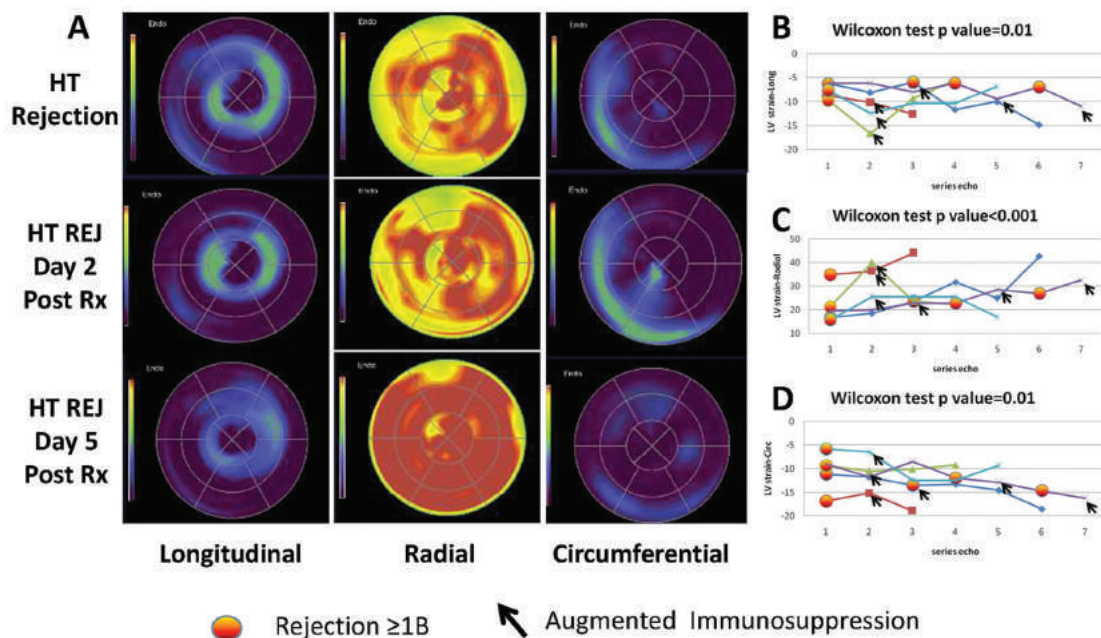


Figure 4. Receiver operating characteristic (ROC) curve analysis for grade 1B or higher rejection. Left ventricular global peak longitudinal strain (GPLS) was an independent parameter for predicting grade 1B or higher rejection ($P = .019$). However, there was no significant difference between global peak radial strain (GPRS) or global peak circumferential strain (GPCS) and the LVEF for diagnosis of grade 1B or higher rejection ($P > .05$). AUC indicates area under the curve.

Figure 5. Changes in LV global longitudinal, radial, and circumferential strain in patients with grade 1B or higher rejection before and after augmented immunosuppression. **A**, Bull’s-eye maps of LV global longitudinal, radial, and circumferential strain in heart transplant (HT) recipients with grade 1B or higher rejection before and after augmented immunosuppression (Rx). **B–D**, The Wilcoxon test showed that longitudinal (**B**), radial (**C**), and circumferential (**D**) global strain values were significantly different before and after augmented immunosuppression.



None of our patients showed ISHLT grade 3B or higher rejection because of the recent progression of immunosuppressive therapy and improvements in care. If not treated early, episodes of acute rejection will lead to more severe and recurrent rejections.³¹ Therefore, the strain analysis described in this study, which could detect ISHLT grade 3A rejection, would be of potential clinical value for monitoring acute rejection in heart transplant recipients.

Our study had several limitations. First, it was a single-center observational and retrospective study. The timing of endomyocardial biopsy and 3D speckle-tracking echocardiography depended entirely on the clinical decisions of physicians. Second, we failed to demonstrate a relationship between the grade of rejection and strain value, which may have been due to the small number of patients and rejections. Therefore, we need to closely investigate a broader range of transplant recipients to help further understand the relationship between LV systolic function and 3D speckle-tracking echocardiographic parameters in these patients.

In conclusion, 3D speckle-tracking echocardiography-derived global peak longitudinal strain is a useful parameter for detecting acute rejection, and an optimal global peak longitudinal strain cutoff value of less than -9.55% can predict grade 1B or higher rejection with high sensitivity and low specificity. Thus, 3D speckle-tracking echocardiography can monitor dynamic and acute rejection ($\geq 1B$) in heart transplant recipients.

References

1. Stehlik J, Edwards LB, Kucheryavaya AY, et al. The registry of the International Society for Heart and Lung Transplantation: 29th official adult heart transplant report—2012. *J Heart Lung Transplant* 2012; 31:1052–1064.
2. Raichlin E, Edwards BS, Kremers WK, et al. Acute cellular rejection and the subsequent development of allograft vasculopathy after cardiac transplantation. *J Heart Lung Transplant* 2009; 28:320–327.
3. Marboe CC, Billingham M, Eisen H, et al. Nodular endocardial infiltrates (Quilty lesions) cause significant variability in diagnosis of ISHLT grade 2 and 3A rejection in cardiac allograft recipients. *J Heart Lung Transplant* 2005; 24(suppl):S219–S226.
4. Baraldi-Junkins C, Levin HR, Kasper EK, Rayburn BK, Herskowitz A, Baughman KL. Complications of endomyocardial biopsy in heart transplant patients. *J Heart Lung Transplant* 1993; 12:63–67.
5. Marie PY, Angioi M, Carreaux JP, et al. Detection and prediction of acute heart transplant rejection with the myocardial T2 determination provided by a black-blood magnetic resonance imaging sequence. *J Am Coll Cardiol* 2001; 37:825–831.
6. Yamamoto S, Bergsland J, Michalek SM, et al. Uptake of myocardial imaging agents by rejecting and nonrejecting cardiac transplants: a comparative clinical study of thallium-201, technetium-99m, and gallium-67. *J Nucl Med* 1989; 30:1464–1469.
7. Angermann CE, Nassau K, Stempfle HU, et al. Recognition of acute cardiac allograft rejection from serial integrated backscatter analyses in human orthotopic heart transplant recipients: comparison with conventional echocardiography. *Circulation* 1997; 95:140–150.
8. Pham MX, Teuteberg JJ, Kfoury AG, et al. Gene-expression profiling for rejection surveillance after cardiac transplantation. *N Engl J Med* 2010; 362:1890–1900.
9. Deng MC, Eisen HJ, Mehra MR, et al. Noninvasive discrimination of rejection in cardiac allograft recipients using gene expression profiling. *Am J Transplant* 2006; 6:150–160.
10. Dodd DA, Brady LD, Carden KA, Frist WH, Boucek MM, Boucek RJ Jr. Pattern of echocardiographic abnormalities with acute cardiac allograft rejection in adults: correlation with endomyocardial biopsy. *J Heart Lung Transplant* 1993; 12:1009–1017.
11. Rosenthal DN, Chin C, Nishimura K, et al. Identifying cardiac transplant rejection in children: diagnostic utility of echocardiography, right heart catheterization and endomyocardial biopsy data. *J Heart Lung Transplant* 2004; 23:323–329.
12. Mondillo S, Maccherini M, Galderisi M. Usefulness and limitations of transthoracic echocardiography in heart transplantation recipients. *Cardiovasc Ultrasound* 2008; 6:2.
13. Sade LE, Sezgin A, Uluçam M, et al. Evaluation of the potential role of echocardiography in the detection of allograft rejection in heart transplant recipients. *Transplant Proc* 2006; 38:636–638.
14. Burgess MI. The role of echocardiography in evaluation of the cardiac transplant recipient. *Minerva Cardioangiol* 2003; 51:677–687.
15. Nitenberg A, Tavolaro O, Benvenuti C, et al. Recovery of a normal coronary vascular reserve after rejection therapy in acute human cardiac allograft rejection. *Circulation* 1990; 81:1312–1318.
16. Sun JP, Abdalla IA, Asher CR, et al. Non-invasive evaluation of orthotopic heart transplant rejection by echocardiography. *J Heart Lung Transplant* 2005; 24:160–165.
17. Stengel SM, Allemann Y, Zimmerli M, et al. Doppler tissue imaging for assessing left ventricular diastolic dysfunction in heart transplant rejection. *Heart* 2001; 86:432–437.
18. Sachdeva R, Malik S, Seib PM, Frazier EA, Cleves MA. Doppler tissue imaging and catheter-derived measures are not independent predictors of rejection in pediatric heart transplant recipients. *Int J Cardiovasc Imaging* 2011; 27:947–954.
19. Haugaa KH, Smedsrud MK, Steen T, et al. Mechanical dispersion assessed by myocardial strain in patients after myocardial infarction for risk prediction of ventricular arrhythmia. *JACC Cardiovasc Imaging* 2010; 3:247–256.
20. Blessberger H, Binder T. Two dimensional speckle tracking echocardiography: basic principles. *Heart* 2010; 96:716–722.

21. Sato T, Kato TS, Komamura K, et al. Utility of left ventricular systolic torsion derived from 2-dimensional speckle-tracking echocardiography in monitoring acute cellular rejection in heart transplant recipients. *J Heart Lung Transplant* 2011; 30:536–543.
22. Marciniak A, Eroglu E, Marciniak M, et al. The potential clinical role of ultrasonic strain and strain rate imaging in diagnosing acute rejection after heart transplantation. *Eur J Echocardiogr* 2007; 8:213–221.
23. Sera F, Kato TS, Farr M, et al. Left ventricular longitudinal strain by speckle-tracking echocardiography is associated with treatment-requiring cardiac allograft rejection. *J Card Fail* 2014; 20:359–364.
24. Kato TS, Oda N, Hashimura K, et al. Strain rate imaging would predict sub-clinical acute rejection in heart transplant recipients. *Eur J Cardiothorac Surg* 2010; 37:1104–1110.
25. Wen H, Liang Z, Zhao Y, Yang K. Feasibility of detecting early left ventricular systolic dysfunction using global area strain: a novel index derived from three-dimensional speckle-tracking echocardiography. *Eur J Echocardiogr* 2011; 12:910–916.
26. Perez de Isla L, Vivas D, Zamorano J. Three-dimensional speckle tracking. *Current Cardiovasc Imaging Rep* 2008; 1:25–29.
27. Billingham ME, Cary NR, Hammond ME, et al. A working formulation for the standardization of nomenclature in the diagnosis of heart and lung rejection. Heart Rejection Study Group. The International Society for Heart Transplantation. *J Heart Transplant* 1990; 9:587–593.
28. Fleiss JL. *The Design and Analysis of Clinical Experiments*. Toronto, Ontario, Canada: John Wiley & Sons; 1986.
29. Pober JS, Jane-Wit D, Qin L, Tellides G. Interacting mechanisms in the pathogenesis of cardiac allograft vasculopathy. *Arterioscler Thromb Vasc Biol* 2014; 34:1609–1614.
30. Torrent-Guasp F, Kocica MJ, Corno AF, et al. Towards new understanding of the heart structure and function. *Eur J Cardiothorac Surg* 2005; 27:191–201.
31. Kubo SH, Naftel DC, Mills RM Jr, et al. Risk factors for late recurrent rejection after heart transplantation: a multiinstitutional, multivariable analysis. Cardiac Transplant Research Database Group. *J Heart Lung Transplant* 1995; 14:409–418.